Zeitschrift: IABSE reports = Rapports AIPC = IVBH Berichte
Band: 54 (1987)

Artikel: Prediction of response of concrete beams and panels by nonlinear finite element analysis
Autor: Balakrishnan, S. / Murray, D.W.
DOI: https://doi.org/10.5169/seals-41946

Prediction of Response of Concrete Beams and Panels by Nonlinear Finite Element Analysis

Prédiction de la résistance de poutres et de panneaux en béton par l'analyse non-linéaire des éléments finis

Vorhersage des Verhaltens von Betonbalken und -Scheiben mittels nichtlineare Finite Element Berechnung

S. BALAKRISHNAN
Senior Engineer
Duthie, Newby, Weber Assoc.
Edmonton, AB, Canada

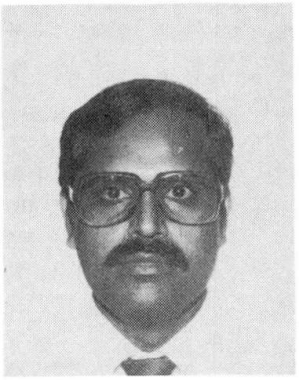

S. Balakrishnan received his Ph.D. degree in Civil Engineering from the Univ. of Alberta, Edmonton, Canada. He has had over 12 years of practical experience in the design of buildings and bridges. His research interests are in the areas of limit and finite element analysis of concrete structures.

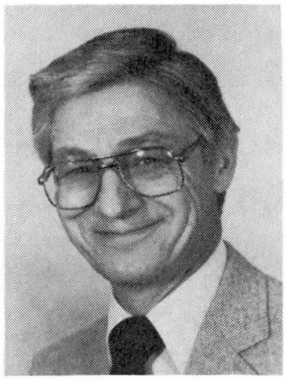

D.W. Murray is a civil engineer holding a B.Sc. from the Univ. of Alberta, Edmonton; a M.Sc. from Imperial College, London; and, a Ph.D. from the Univ. of California, Berkeley. He has been a member of the academic staff at the Univ. of Alberta since 1960.

D.W. MURRAY
Professor
Univ. of Alberta
Edmonton, AB, Canada

SUMMARY
In order for practising engineers to have confidence in the use of NLFEA (Nonlinear Finite Element Analysis) for concrete, there is a need for verification that the method gives results which consistently agree with test data on beams and panels exhibiting various failure modes. In this paper, finite element formulations are presented, and a simple constitutive relationship is described, which have been found to be effective in predicting behavior for a wide range of beams and panels.

RÉSUMÉ
Afin de permettre aux ingénieurs praticiens d'avoir confiance dans l'utilisation de l'analyse par méthode des éléments finis non-linéaires pour le béton, il faut vérifier que cette méthode donne des résultats qui sont en accord permanent avec des résultats d'essais sur des poutres et des panneaux ayant subi des dommages divers. La formulation par éléments finis est présentée; la relation constitutive simple décrite a permis de prévoir le comportement réel d'un grand nombre de poutres et de panneaux.

ZUSAMMENFASSUNG
Der Vergleich mit Versuchsresultaten soll dem Ingenieur in der Praxis Vertrauen in nichtlineare FE-Analysen (NLFEA) geben. Der Beitrag gibt FE-Formulierungen und einfache Werkstoffgesetze, die sich bei vielen Balken- und Scheibentragwerken bewährt haben.

1. INTRODUCTION

The vast majority of global structural analyses in engineering offices follow traditional patterns - linearized, simplified models in which the reinforced concrete system is assumed to be uncracked, homogeneous and isotropic. The internal forces and moments calculated from these models are then used to design the members based on ultimate strength using the code provisions which in turn have been based on simplified models and synthesis of experimental data. Special and complex structural problems are often solved using intuitive judgement and/or tests on small scale models. Even plasticity based methods involve assumptions regarding the material behavior and the use effectiveness factors to correlate with experimental data.

The finite element method (i.e., FEM), because of its ability to take into account the conditions of equilibrium, compatibility and nonlinear material behavior, is a valuable analytical tool which can be used to: (1) directly predict the structural response in the entire load range up to failure; (2) gain greater understanding of the behavior so that simpler but realistic models can be developed; and, (3) study the effects of important parameters on member behavior thus providing a firmer basis for code provisions.

However, in order for practicing engineers to have confidence in the FEM, there is a need for verification that the method gives results which consistently agree with experimental data for a wide range of geometric and material parameters. Often general purpose codes which purport to have the capability of nonlinear concrete analysis have proved to be a disappointment to practitioners. There is little point to a code which can properly predict flexural failure if it predicts such a failure when the true structural failure is a shear failure.

Also, in order for the practicing engineer to use the nonlinear FEM, the cost and time constraints must not be exceeded. The cost and time involved in the application of the nonlinear FEM must be competitive with other possible approaches, such as testing programs, or perhaps just using a larger factor of safety in design. Thus there is a need to determine the influence of various parameters used in the numerical analysis in predicting the behavior so that individual analyses can be tuned to the desired accuracy.

2. OBJECTIVES

The objectives of this paper are:

1. to describe a simple constitutive relationship for concrete which the authors have found to be effective in the solution of plane stress modeling of beams [1] and panels [2];

2. to demonstrate the applicability of the models by comparing the predicted behavior to the behavior observed in the laboratory for specimens exhibiting various types of failure modes;

3. to present the authors' experience with respect to the effects (on the analysis) of various material parameters and their importance relative to the various failure modes.

3. FINITE ELEMENT FORMULATIONS

A typical finite element model used by the authors for a beam structure is composed of quadratic serendipity concrete elements, embedded primary reinforcing steel, and distributed bond elements selectively placed along the reinforcement [1]. Where bond elements are included, nodal points along the

reinforcement layer, each with a single slip degree of freedom, must be added.

The formulation of isoparametric elements is available in the literature (see, for example [3], [4]). The formulations for the embedded reinforcement and bond elements are presented in [1] and summarized briefly in the following.

The the authors' knowledge, all embedded and distributed representations for reinforcement that are currently available in literature assume perfect bond between steel and concrete. An embedded reinforcement formulation including bond-slip is developed herein. Such a formulation obviates the need for locating the reinforcing element nodal points at the solid element boundaries.

The virtual work of a reinforcing element is given by

$$\sum_{m} \int \delta\varepsilon_s \sigma_s A_s dr$$

where A_s is the cross-sectional area of reinforcement; dr is the differential length; ε_s is the strain in reinforcement and σ_s is the stress in reinforcement. Considering the reinforcing element, as shown in Fig. 1, the steel displacement w_s at any point of the element in a direction tangential to the reinforcing bar is written as

$$w_s = w_c + w_b \qquad (3.1)$$

where w_c is the displacement of the concrete at that point as interpolated from nodal displacements and w_b is the bond slip (i.e. the relative displacement between the steel and the concrete).

From Fig. 1,

$$w_c = u \cos\theta + v \sin\theta \qquad (3.2)$$

Let $U_{b_1}, U_{b_2} \ldots U_{b_p}$ be p slip degrees of freedom of p nodes located on the reinforcement within the element.
Then,

$$w_b = \sum_{j=1}^{p} H_j U_{b_j} \qquad (3.3)$$

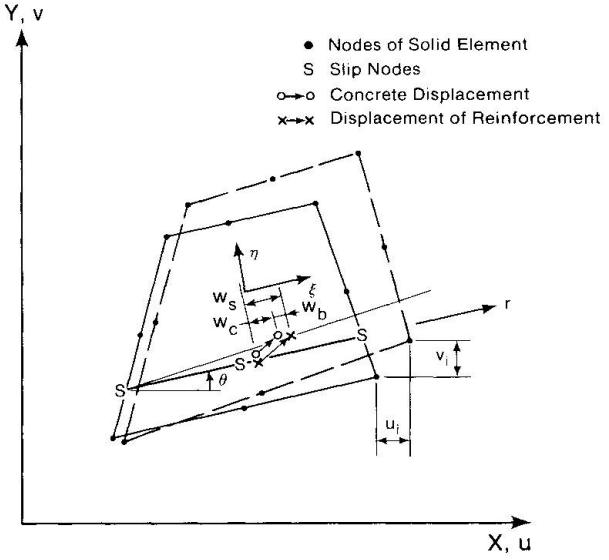

Fig. 1. Displacements for Embedded Bond Elements

where H_j are the shape functions used to interpolate the bond slip at any point. The strain in the reinforcing steel at any point is

$$\varepsilon_s = \frac{dw_s}{dr} \qquad (3.4)$$

From Eqs. 3.1, 3.2 and 3.4, and assuming that θ does not vary along the element,

$$\varepsilon_s = \frac{du}{dr}\cos\theta + \frac{dv}{dr}\sin\theta + \frac{dw_b}{dr} \qquad (3.5)$$

Considering for simplicity that the reinforcing element is placed parallel to a natural coordinate axis, say the ξ axis, the relationships

$$du = \frac{\partial u}{\partial \xi} d\xi + \frac{\partial u}{\partial \eta} d\eta \quad ; \quad dv = \frac{\partial v}{\partial \xi} d\xi + \frac{\partial v}{\partial \eta} d\eta \tag{3.6}$$

will reduce Eq. (3.5) to

$$\varepsilon_s = \frac{1}{J_s} \langle \cos\theta \quad \sin\theta \rangle \begin{bmatrix} \langle \frac{\partial N_i}{\partial \xi} \rangle & \langle 0 \rangle \\ \langle 0 \rangle & \langle \frac{\partial N_i}{\partial \xi} \rangle \end{bmatrix} \begin{Bmatrix} u_i \\ v_i \end{Bmatrix} + \frac{1}{J_s} \langle \frac{dH_j}{d\xi} \rangle \{U_{b_j}\} \tag{3.7}$$

wherein u_i, v_i are the nodal displacements, i = 1, 2, ... q; q = the total number of nodes for the solid element; N_i = the shape functions; j = 1, 2, ... p; and $J_s = \sqrt{\left(\frac{dx}{d\xi}\right)^2 + \left(\frac{dy}{d\xi}\right)^2}$.

The stiffness matrix for the reinforcing element is formed and assembled in the standard manner using Eq. 3.7 to describe the steel strain, and added to the stiffness matrix of the solid element.

The virtual work of the bond element is given by

$$V.W._{bond} = \delta \langle U_{b_j} \rangle \left[\sum_{m} \int_{-1}^{1} \{H_j\} D_b \langle H_j \rangle A_p J_s d\xi \right] \{U_{b_j}\} \tag{3.8}$$

where D_b is the bond stress producing unit slip, m is the number of bond elements in the solid element and A_p is the contact area per unit length of reinforcing steel. The factor in the brackets in the Eq. 3.8 is the stiffness matrix for the bond elements and is assembled with the solid and reinforcement element matrices in the standard manner.

4. CONSTITUTIVE MODEL

The approach taken herein is to attempt to find the simplest possible constitutive model that can capture those essential characteristics of reinforced concrete behavior which are necessary in order to reliably reproduce basic types of observed failure modes for a limited class of structures, namely, net reinforced concrete panels and reinforced concrete beams. Reliability of the model to achieve this result is the paramount consideration.

The model is intended for use in a 'smeared cracking' type of finite element analysis. A more detailed description of the constitutive model is given in [5]. It has a piecewise linear uniaxial stress-strain relationship, with tension softening and tension stiffening for tensile response, and strain

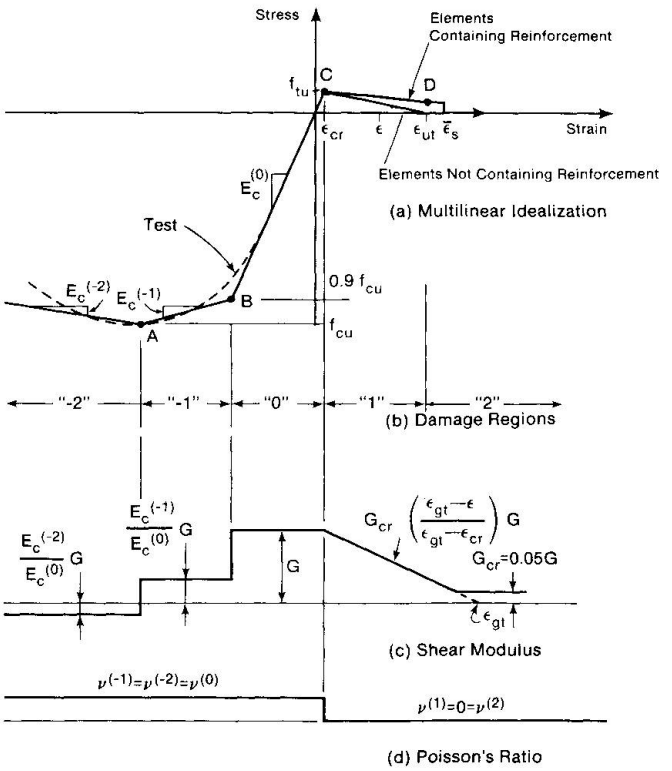

Note: superscripts in parentheses denote damage regions.

Fig. 2. Assumed Strain Dependence of Concrete Properties

hardening and strain softening for compressive response, as shown in Fig. 2. The points of slope discontinuity of the uniaxial curve divide the idealized stress-strain response curve into regions referred to as 'damage regions'. These also are shown in Fig. 2.

When used under biaxial stress conditions the model is considered orthotropic after cracking and the direction of cracking dictates the orientation of the orthtropic axes. The shear stiffness is considered to be piecewise linear and may be discontinuous between damage regions as indicated in Fig. 2. The peak values of the stress-strain curve under biaxial stress conditions are adjusted to those associated with the 'failure envelope' of Fig. 3, which is a modification of the Kupfer-Hilsdorf failure curve. The modification is in the tension-compression stress space and consists of the separate specification of the compressive and tensile failure curves. For load path OA in Fig. 3, the cracking occurs at A and the post-cracking compressive strength is given by the abcissa of B where AB is a horizontal line.

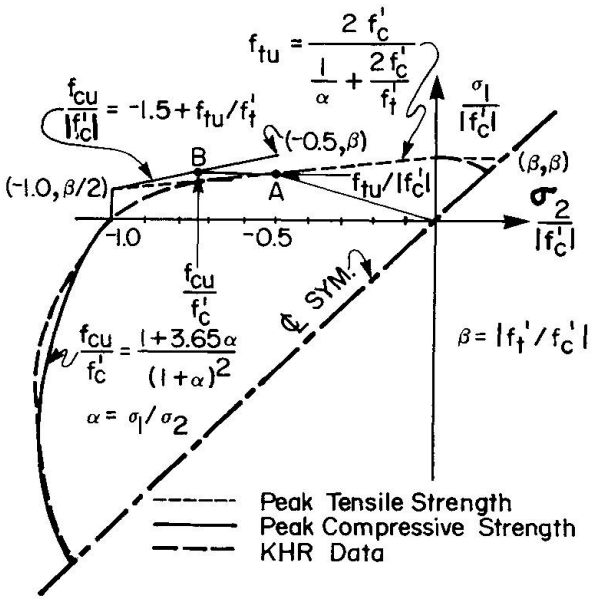

Fig. 3. Peak Strength Envelopes in Biaxial Stress Space

In the undamaged region, i.e., region "0" of Fig. 2, the constitutive relationship is considered isotropic and the incremental biaxial stress strain relationship is given by

$$\begin{Bmatrix} d\sigma_1 \\ d\sigma_2 \\ d\tau_{12} \end{Bmatrix} = \frac{E_c^{(0)}}{1 - \nu^2} \begin{bmatrix} 1 & \nu & 0 \\ \nu & 1 & 0 \\ 0 & 0 & \frac{1-\nu}{2} \end{bmatrix} \begin{Bmatrix} d\varepsilon_1 \\ d\varepsilon_2 \\ d\gamma_{12} \end{Bmatrix} \qquad (4.1)$$

with respect to any set of reference axes. Poisson's ratio is assumed constant as shown in Fig. 2.

Cracking is assumed to occur on the plane of maximum principal stress when this maximum principal stress reaches the dotted line of Fig. 3. The material is then assumed to be orthotropic with the axes of orthotropy parallel and orthogonal to the crack. Poisson's ratio is set to zero when cracking is initiated, and Eq. 4.1 becomes

$$\begin{Bmatrix} d\sigma_1 \\ d\sigma_2 \\ d\tau_{12} \end{Bmatrix} = \begin{bmatrix} E_c^{(1)} & 0 & 0 \\ 0 & E_c^{(k)} & 0 \\ 0 & 0 & G_{cr} \end{bmatrix} \begin{Bmatrix} d\varepsilon_1 \\ d\varepsilon_2 \\ d\gamma_{12} \end{Bmatrix} \qquad (4.2)$$

in which k indicates the damage region. The response in the two in-plane orthotropic directions is, therefore, uncoupled. Equations 4.1 and 4.2 have been used effectively with a 'fixed crack technique' for beams [1] and a 'rotating crack technique' for orthogonally reinforced elements [2].

In the rotating crack model, as adapted by the authors, the axes of orthotropy are assumed to coincide with the principal strain axes (total strains up to the previous iteration) even after cracking, whereas in the fixed crack model the axes of orthotropy are fixed parallel and perpendicular to the crack at the onset of cracking. The rotating crack model is used for orthogonally reinforced elements where it has been shown both theoretically [6,7] and experimentally [8] that crack direction may change, at least in an average sense. The fixed crack model is used for elements containing no reinforcement or reinforcement in one direction only, where appreciable crack rotation may not occur.

Two interrelated phenomena associated with cracking, namely 'tension softening' at the cracks, and the 'tension stiffening' effect of intact concrete segments between the macro cracks, should be taken into consideration in the determination of $E_c^{(1)}$, the post-cracking strain softening modulus. Tension softening is related to the fracture energy release rate (i.e. energy expended in the formation of a unit area of a crack, G_f for mode I cracking) by

$$\varepsilon_{ut} = \frac{2\,G_f}{f'_t\,S} \tag{4.3}$$

where ε_{ut} is the strain at which the normal stress at crack interface has reduced to zero (Fig. 2), S is the crack spacing and f'_t is the peak tensile stress as determined from a split cylinder test.

The tension stiffening is dependent on the crack spacing, reinforcement ratio and bond slip characteristics of the steel/concrete interface. Assuming a bilinear concrete stress variation and an incipient crack about to form midway between two macrocracks, tension softening and tension stiffening are combined [5] to produce the relationship

$$\sigma_t = \frac{f_{tu}}{2}\left\{1 + \frac{\varepsilon_{ut} - \varepsilon}{\varepsilon_{ut} - \varepsilon_{cr}}\right\} \quad \text{for} \quad \varepsilon_{cr} < \varepsilon < \varepsilon_{ut} \tag{4.4a}$$

and

$$\sigma_t = \frac{f_{tu}}{2} \quad \text{for} \quad \varepsilon > \varepsilon_{ut} \tag{4.4b}$$

The shear modulus of cracked concrete is dependent on the crack width and therefore, in a smeared crack approach, on the tensile strain. In order to account for dowel action and for numerical stability, G_{cr} is always taken to be greater than or equal to 5% of the uncracked concrete shear modulus. The value to be used for ε_{gt}, shown in Fig. 2, depends on the expected crack spacing and crack width. Based on numerical studies [1,2] it was found that for beams ε_{gt} of Fig. 2 can be taken to be equal to ε_{ut} whereas for net-reinforced panels (in which cracks are finer and more distributed) a value between 0.005 and 0.01 appears satisfactory.

It has been recognized that when strain localization occurs, standard tests no longer measure the fundamental material properties, but rather the structural system under test. (See, for example, [9].) Therefore, the strain softening modulus in compression should be related to the mesh size and the degree of confinement. At the present time, no reliable method appears to be available to relate the element size to a 'homogenized' compressive strain softening modulus. Again, based on numerical studies, a value of -0.05E is recommended for beams without web reinforcement. For beams with confining reinforcement, the expression in [10] was found to yield good results.

5. APPLICATION TO REINFORCED CONCRETE PANELS

The load-deformation behavior of orthotropically reinforced panels is characterized by significant changes in the orientation of the principal axes and reduction in stiffness after concrete cracks. The three major failure modes of the panels are: (1) ductile failure by both layers of steel yielding, designated as the 'D' mode of failure herein; (2) brittle failure by crushing of concrete in compression, designated as the 'B' mode herein; and (3) crushing of concrete after one layer of steel yields, denoted as the 'DB' mode herein.

The rotating crack model was used, in conjunction with the constitutive relationships and the post-cracking compressive strength criterion described in Section 4, to predict the behavior of some of the panels tested by Vecchio and Collins [8]. The results are summarized in Table 1. Comparison to the experimental results is shown in Fig. 4. The prediction using the empirical relationships of Vecchio and Collins [8] is also shown in Fig. 4. Panels PV4 and PV11 failed in the 'D' mode; Panels PV10, PV19, PV21 and PV29 failed in the 'DB' mode; Panels PV23, PV25 and PV27 failed in the 'B' mode. Panels PV19, PV27, PV25 and PV29 were the subject of an international competition [11].

It is seen that the failure load and the global stress-strain predictions using the FEM are reasonably accurate. The failure mode has been correctly predicted in all cases. Failure loads for panels failing in the D or DB modes have been accurately predicted using the FEM and are close to those obtained using plasticity based methods [12]. Failure loads of panels failing in the B mode have been somewhat underestimated, mainly due to the underestimation of the tension stiffening contribution. Panels PV27 and PV23 contain the same reinforcement ratio and were made of concrete of the same cylinder compressive strength but PV27 was loaded in pure shear whereas PV23 was loaded in biaxial compression in addition to shear. The FEM predicts an increased shear strength for Panel PV23 due to the action of compressive stresses.

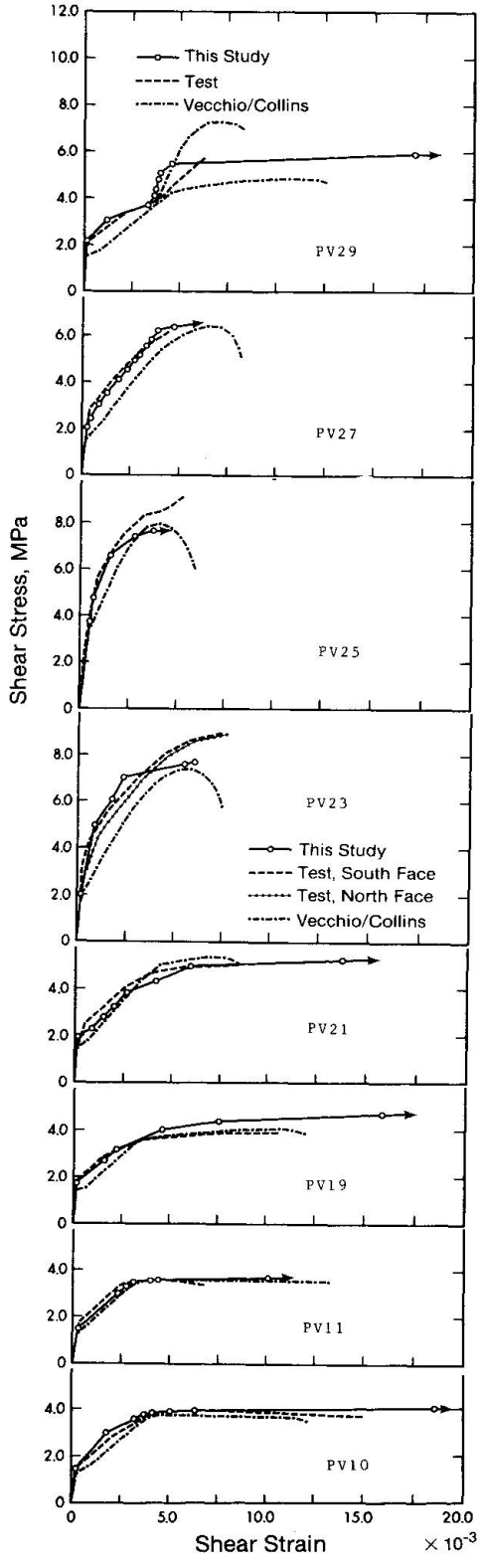

Fig. 4. Comparison with Tests for Vecchio/Collins Panels

Panel	Loading Condition $\tau:f_x:f_y$	Steel Reinforcement X Direction ρ_x	f_{sx} MPa	Y Direction ρ_y	f_{sy} MPa	Concrete f'_c MPa	Experimental† Failure Mode	Failure Load MPa	FE Prediction Failure Mode	Failure Load MPa	Experimental / Finite Element
PV4	1:0:0	.01056	242	.01056	242	26.6	D	2.89	D	2.60	1.11
PV10	1:0:0	.01785	266	.00999	276	14.5	DB	3.97	DB	4.00	0.99
PV11	1:0:0	.01785	235	.01306	235	15.6	D	3.56	D	3.60	0.99
PV19	1:0:0	.01785	458	.00713	299	19.0	DB	3.95	DB	4.45	0.89
PV21	1:0:0	.01785	458	.01296	302	19.5	DB	5.03	DB	5.20	0.97
PV23	1:-0.39:-.39	.01785	518	.01785	518	20.5	B	8.87	B	7.60	1.17
PV25	1:-.69:-.69	.01785	466	.01785	466	19.2	B	9.12	B	7.70	1.18
PV27	1:0:0	.01785	442	.01785	442	20.5	B	6.35	B	6.25	1.02
PV29	1:0:0 1:-1:-1	.01785	441	.00885	325	21.7	DB	5.87	DB	5.90	1.0

† Ref. [8]
D - Both x and y direction reinforcement yielded at failure.
DB - Y direction reinforcement yielded; X direction reinforcement not yielded, concrete crushing failure.
B - Neither reinforcement layer yielded at failure; concrete crushing failure.

Table 1. Finite Element Prediction of Panel Failure

Panel PV29 was loaded in pure shear until one layer of reinforcement yielded. Subsequent shear loading was accompanied by the application of biaxial compressive stresses of equal magnitude. The fact that the behavior of this panel has been predicted with reasonable accuracy shows that the FEM and the post cracking compressive strength criterion as developed herein may be used for nonproportional loading.

6. APPLICATION TO REINFORCED CONCRETE BEAMS

The principal modes of failure in R/C beams are: (1) ductile flexural failure by yielding of primary reinforcement, (2) diagonal shear failure of beams without web reinforcement, (3) shear-compression failure of beams with web reinforcement, (4) compressive failure of concrete in over-reinforced beams, (5) brittle failure of 'compression struts' in deep beams, and (6) 'local' failure such as bearing failure and anchorage bond failure.

The 'fixed crack model', in conjunction with the constitutive relationship described in Section 3, was used to predict the behavior of a number of beams exhibiting the different failure modes described above. Table 2 lists some of the beams analyzed and Figs. 5, 6 and 7 show their load-deflection behavior. Fig. 5 illustrates a flexural failure, Fig. 6 illustrates shear failures and Fig. 7 illustrates bearing and compressive strut failures.

In most nonlinear finite element analyses the failure load is assumed to have been reached when there is failure of convergence of force and/or displacement vector norms, or if the tangent stiffness matrix contains a zero or negative element on the diagonal. The corresponding load is referred to as the collapse load although it might be the numerical procedure that has failed and not the structure. Thus, it is important to confirm that failure of the structure has in fact occurred and to determine the mode and causes of failure.

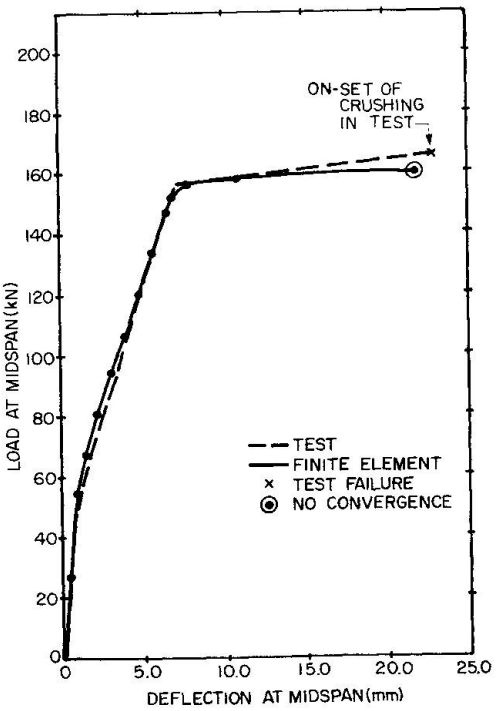

Fig. 5. Comparison with Tests for Beam Flexural Failure

Beam[7]	Reference	Failure[8] Mode	a/d	Web Reinforcement?	Span m	Depth mm	Reinforcement %	Load in Test kN	Load by NLFEA kN	Test Load / NLFEA Load
BUS J-4	[13]	SY	4.33	No	3.96	457	1.09	167	160	1.044
BRS 0A1	[14]	DT	3.97	No	3.66	461	1.81	334	343	0.974
BRS 0A2	[14]	DT	4.90	No	4.57	466	2.27	356	356[1] 400[2]	1.000
BRS 0A3	[14]	DT	6.94	No	6.40	461	2.74	37.8	400	0.945
BRS A1	[14]	SC	3.92	Yes	3.66	466	1.80	467	427	1.094
BRS A2	[14]	SC	4.93	Yes	4.57	464	2.28	489	445	1.099
BRS A3	[14]	FC	6.91	Yes	6.40	466	2.73	467	511	0.914
ROM 1/1.0	[15]	CS	1.0	No	2.0	950	0.95	1204[3] 1398[4]	1180[5] 1200[6]	1.093
LEW WT3	[16]	BF	0.5	Yes	1.44	1385	0.29	1290	1216	1.061

Mean = 1.025

(1) Based on relative vertical displacement
(2) Based on failure of convergence
(3) Compressive failure on North end
(4) Compressive failure on South end
(5) Quadratic elements
(6) Bilinear elements
(7) BUS = Burns-Siess
BRS = Bresler-Scordelis
ROM = Rogowski-MacGregor
LEW = Leonhardt-Walther

(8) Failure Mode Notation
SY = Flexural failure by steel yielding
DT = Diagonal tension failure
SC = Shear compression failure
FC = Flexural compression failure
CS = Compressive strut failure
BF = Bearing failure

Table 2. Finite Element Prediction of R/C Beam Behavior

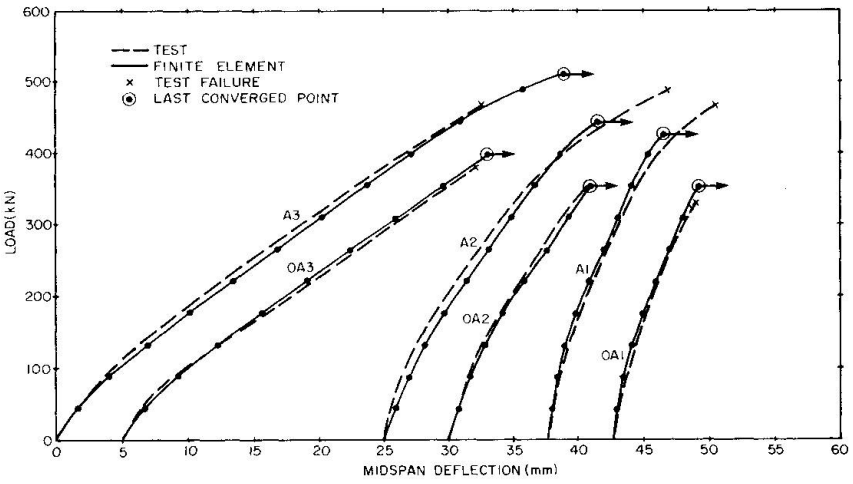

Fig. 6. Comparison with Tests for Beam Shear Failures

A number of failure 'indicators' may be used for this purpose. Details of these indicators are described elsewhere [1,17]. However, a short description of the most important is as follows.

The failure mode of beams failing by primary steel yielding can be simply verified by steel and concrete stresses and strains at the final load step. For shear critical beams without web reinforcement, the indicators are: (1) the relative vertical displacement (sometimes referred to as 'thickening' [14]) between the top and bottom faces of the beam shows marked increase before failure, Fig. 8; (2) the shear strains tend to be of the same order of magnitude as normal strains, Fig. 9; (3) steel and concrete flexural stresses are well below their maximum values; and, (4) the crack pattern shows cracking near the neutral axis in an almost horizontal direction and extending into the compression region, Fig. 10. For beams failing in diagonal compression (i.e failure of a compressive strut), the compressive stress plot as shown in Fig. 11 gives an indication of the failure mode.

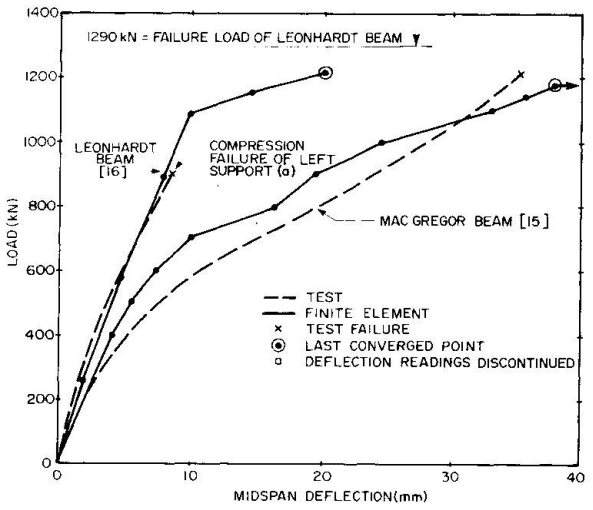

Fig. 7. Comparison with Tests for Bearing and Strut Failures

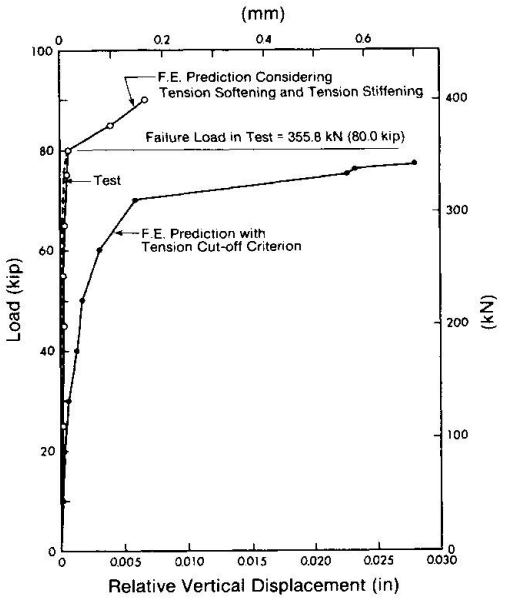

Fig. 8. Detection of Beam Shear Failure by Thickening

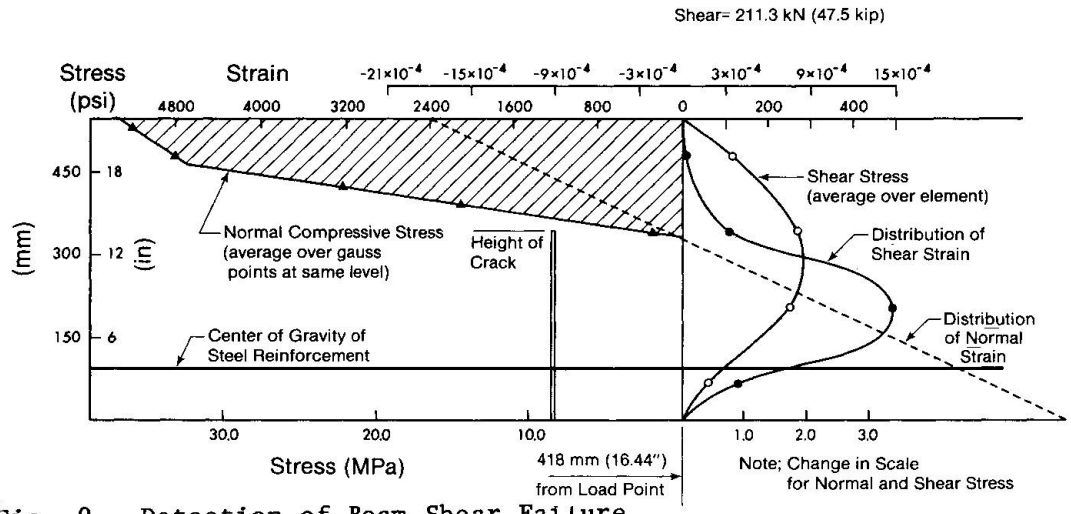

Fig. 9. Detection of Beam Shear Failure by Shear Strain

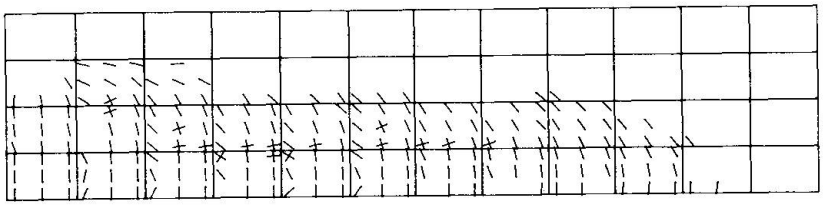

Fig. 10. Detection of Beam Shear Failure by Cracking

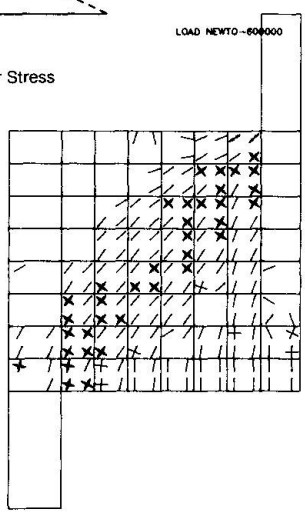

Fig. 11. Diagonal Strut Compression Failure

7. INFLUENCE OF MATERIAL PARAMETERS ON THE FAILURE PREDICTION

In the authors' experience, the predicted response is often insensitive to the precise values of the parameters required to describe the curves of Fig. 2 and 3. However each feature of these curves is important in predicting some aspect of behavior as various failure modes appear. For example, a tension cut-off criterion failed to predict satisfactorily the failure load and failure mode of shear critical beams. For this class of beams, it is also important to adequately represent the dependency of shear stiffness of cracked concrete on crack width (i.e., on crack strain in smeared crack analysis). The use of a constant shear retention factor leads to failure predictions which are highly dependent on the actual factor adopted. For beams failing in shear-compression, such as those containing high web reinforcement ratios, and for panels failing before steel yielding, the compressive strain hardening and softening moduli significantly influence the failure mode and failure load. The post-cracking compressive strength of concrete has a major influence on the failure load of deep beams and panels with high reinforcement ratios.

8. CONCLUSIONS

1. The major conclusion of the study reported in this paper is that the finite element method can be used to closely predict the behavior of reinforced concrete members subjected to in-plane forces if proper care is taken in modeling the material characteristics. The load deflection behavior, crack pattern, failure load and failure mode can be predicted with an accuracy that is acceptable for engineering purposes.

2. In order to obtain reliable predictions, it appears to be necessary to properly include consideration of major sources of nonlinearity in reinforced concrete, namely: tension softening and tension stiffening; compressive strain hardening and strain softening; variation of shear modulus with crack width; and, bond slip between steel and concrete. For proper 'homogenization' of these material properties, structural details and response characteristics must be included in their determination. This requires that the analyst be knowledgeable about how the behavior of the structure will affect these properties. Techniques of estimating these properties are given in [1], but are not included herein because of space limitations. More detailed descriptions of the analyses will appear subsequently in the literature [2,5,17].

9. REFERENCES

1. BALAKRISHNAN, S. and MURRAY, D.W., Finite Element Prediction of Reinforced Concrete Behavior, Structural Engineering Report No. 138, Department of Civil Engineering, University of Alberta, July 1986.

2. BALAKRISHNAN, S. and MURRAY, D.W., Prediction of RC Panel Behavior by NLFEA, Submitted for publication to the Journal of Structural Engineering, ASCE, New York, 1987.

3. BATHE, K.J., Finite Element Procedures in Engineering Analysis, Prentice-Hall, Englewood Cliffs, New Jersey, 1982.

4. ZIENKIEWICZ, O.C., The Finite Element Method, McGraw-Hill Book Company (UK) Ltd., London, 1977.

5. BALAKRISHNAN, S. and MURRAY, D.W., Concrete Constitutive Model for NLFE Analysis of Structures, Submitted for publication in the Journal of Structural Engineering, ASCE, New York, N.Y., 1987.

6. GUPTA, A.K. and HABIBOLLA, A., Changing Crack Direction in Reinforced Concrete Analysis, Report, Dept. of Civil Engineering, North Carolina State University, Raleigh, 1982.

7. COPE, R.J. and RAO, P.V., Non-linear Finite Element Strategies for Bridge Decks, IABSE Colloquium on Advanced Mechanics of Reinforced Concrete, Delft, 1981.

8. VECCHIO, F.J. and COLLIS, M.P., Response of Reinforced Concrete to In-Plane Shear and Normal Stresses, Publication No. 82-03, Department of Civil Engineering, University of Toronto, March 1982, 332 p.

9. DE BORST, R., Nonlinear Analysis of Frictional Materials, Doctoral Thesis, Delft University of Technology, Delft, The Netherlands, 1986.

10. VALLENAS, J., BERTERO, V.V. and POPOV, E.P., Concrete Confined by Rectangular Hoops and Subjected to Axial Loads, Report No. UCB/EERC-77/12, University of California, Berkeley, 1977.

11. COLLINS, M.P., VECCHIO, F.J. and MELHORN, G. An International Competition to Predict the Response of Reinforced Concrete Panels, Canadian Journal of Civil Engineering, Vol. 12, No. 3, 1985, pp. 624-644.

12. NIELSEN, M.P., Limit Analysis and Concrete Plasticity, Prentice-Hall Inc., New Jersey, 1984.

13. BURNS, N.H. and SIESS, C.P., Repeated and Reversed Loading in Reinforced Concrete, ASCE Journal of the Structural Division, Vol. 92, ST5, 1966, pp. 65-78.

14. BRESLER, B. and SCORDELIS, A.C., Shear Strength of Reinforced Concrete Beams, ACI Journal, Vol. 60, NO. 1, 1963, pp. 51-73.

15. ROGOWSKY, D.M., MACGREGOR, J.G., and ONG, S.Y, Tests of Reinforced Concrete Deep Beams, ACI Journal, Proceedings, Vol. 83, No. 4, 1986, pp. 614-623.

16. LEONHARDT, F. and WALTHER, R., Wandertige Trager, Report, Deutscher Ausschuβ für Stahlbeton, Heft 178, Berlin, 1966.

17. BALAKRISHNAN, S., ELWI, A.E. and MURRAY, D.W., Application of FEM to Predict Concrete Beam Behavior, to be submitted to the Journal of Structural Engineering, ASCE, New York, 1987.